

LATERAL BEHAVIOR OF POST-TENSIONED CROSS LAMINATED TIMBER WALLS USING FINITE ELEMENT ANALYSIS

Zhouyan Xia¹, Jan Willem van de Kuilen²

ABSTRACT: Cross laminated timber (CLT) has been rapidly developed and utilized for multi-rise constructions in recent years, even high-rise CLT buildings with 40 stories have been proposed and designed. A use of unbonded post-tensioning (PT) steel bars through over CLT walls of the high-rise CLT buildings to take up the tensile forces produced by wind load has been considered, following the regulations of unbonded post-tensioned (UPT) concrete walls. This paper introduces a finite element model to simulate the nonlinear lateral load behavior of the UPT high-rise CLT buildings with elastic connections between the CLT elements. The analysis results indicate that the unbonded PT bars can effectively reduce the lateral displacement of the high-rise CLT building. While compared with a theoretical full rigid CLT model, the advanced model is found to be more accurate for estimating the response of UPT high-rise CLT building under horizontal load.

KEYWORDS: Cross laminated timber (CLT), High-rise CLT building, Unbonded post-tensioning, Lateral behavior.

1 INTRODUCTION

Cross laminated timber (CLT) is now widely accepted by the markets of Europe, Australia and to a lesser extent North America. Benefitting from its advantages, such as large panel size, high strength-to-weight ratio, short on-site construction time and environmental impact, CLT provides a cost-effective alternative to conventional structural solutions. Until today CLT has been used in buildings up to ten stories [1]. At this level some difficult to quantify questions arise about the possibility of even higher building with more complex requirements with regard to fire, horizontal displacement, building core construction, etc. In view of this tendency, some design issues, including mechanical properties, fire safety, geometry, structural form and etc., for tall timber buildings up to 20 stories [2] have been identified. Design challenges are various and some aspects have been addressed by proposing possible solutions using a mix of timber and concrete in a high-rise building concept using outriggers and vertical tension elements inside the CLT elements in the facade [3]. Preliminary calculations showed that from a mechanical viewpoint it should be possible to build such a building.

Besides the overall structural system design, the connection stiffness of CLT construction is another

essential issue. Traditional concrete is fully rigid, while CLT connections need to be modelled appropriately, in order to be able to assess the building stiffness reliably. It is known that the multi-rise CLT buildings normally use conventional fasteners to integrate the panels into a complete structure with the advantages of easy handling and simple installation. Basically, hold-downs, angle brackets and screws are available for the connections to resist the lateral loads caused by earthquakes [4-6].

For tall buildings, one of the vital considerations in design is the structural performance under wind load. Particularly for CLT tall buildings, they are more sensitive to wind load due to the lightweight CLT material. As in this paper a comparative analysis is performed between a realized concrete building in Shanghai and an equivalent building with CLT. As the building lay-out has not been altered considerably, a comparative analysis about the stiffness is possible. Therefore, the strength of CLT shear walls, which are the primary lateral load resisting members for CLT construction system, has to be improved. More specifically, the focus should be on strengthening the connections between CLT elements.

Referring to the experience from PRESSS (PREcast Seismic Structural Systems) research program [7, 8], unbonded post-tensioned (UPT) wall system, which is used to strengthen and stiffen precast concrete system, could also be a solution for the connection system of high-rise CLT buildings. This paper looks into the application of vertical prestressing to CLT walls. As horizontal loads prevail in tall building, uplifting is to be avoided and

¹ Zhouyan Xia, Holzforschung München, Technische Universität München, 45 Winzererstr., Munich, Germany. Email: xia@hfm.tum.de

² Jan Willem Van de Kuilen, HFM, TU München, Germany & TU Delft, Netherlands.

prestressing can be a helpful tool. In order to predict the lateral behavior of unbonded post-tensioned CLT walls, a nonlinear finite element model, using the software SAP2000® version 16, has been developed. The obtained numerical analysis data provides reference information and experience for the width to height ratios of tall wooden buildings on the basis of CLT.

2 UNBONDED POST-TENSIONED CLT HIGH-RISE BUILDINGS

2.1 STRUCTURE DESIGN

In the preliminary design of the 40-story CLT buildings [3], the structural system consisted of a concrete central core to resist the major lateral loads, and concrete outriggers to include a number of additional functions, including the possibility of having tensile bars in the facade. In this paper, the whole building is made of CLT to see the influence of CLT panels having substituted the concrete core. While the outriggers are still made of concrete, the overall structural behaviour is now determined mainly by CLT and the prestressing effects. Larger deformations are consequently expected when comparing the building with a full concrete core. In order to restrain the building from too much sway, an analysis is performed using an unbonded post-tensioning system inside the vertical walls as a potential solution. Such a solution has been also applied in the Linnologen project in Växjö, Sweden [9, 10].

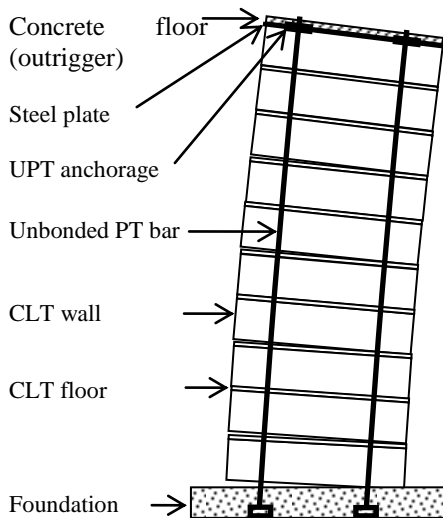


Figure 1: Unbonded post-tensioned CLT wall under lateral loads

By applying unbonded PT steel in CLT wall, the system is quite similar as applied in precast concrete elements. As an example shown in Figure 1, a ten-story CLT wall is integrated by high strength PT bars that are not bonded to the CLT panels. The bars are placed inside oversize ducts that are embedded previously in CLT panels. In this case,

the steel section and the desired stress are transferred to CLT wall only through end anchorages and stiffeners. The unbonded UP bars are highly stressed and connected to the wall only at the end bearing plates. Horizontal joints between the wall panels and floor slabs are still conventional angle brackets.

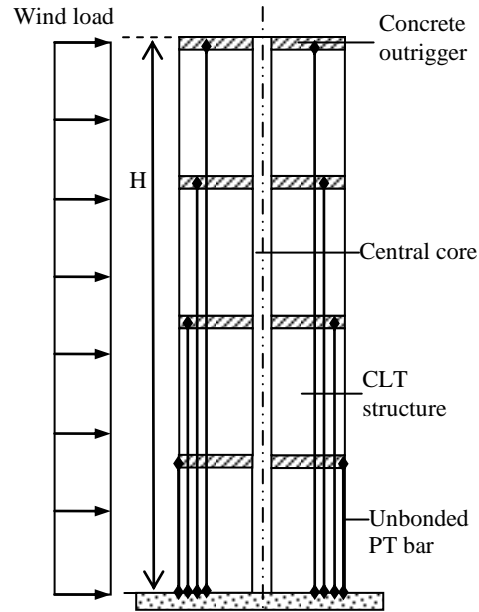


Figure 2: Example of a tall CLT building with four concrete outriggers

The 40-story CLT building is arbitrarily separated into four levels of ten stories each, based on the outriggers that are evenly located along the height of the building [11], i.e. every tenth story (Figure 2). CLT core walls and sidewalls are both required to carry tensile stresses under lateral load conditions. Four groups of unbonded PT bars, as illustrated in Figure 2, are therefore installed in these walls to provide compressive stress. The idea is to avoid tensile loading between the CLT panels in any of the possible load cases. The unbonded PT bars are fixed at the foundation and anchored at corresponding outriggers. Consequently, they are instead of original vertical joints, i.e. hold-down brackets, between CLT walls. This results in more efficient material utilizing and reducing congestion.

In addition to decreasing the required number of connectors, a post-tensioning system has the potential to provide sufficient restoring force to regulate the building back to its initial position. This characteristic is recognized as “self-correcting” [12, 13]. It can reduce the residual lateral displacement of the wall after large wind load or earthquake actions. Compared to conventional hold-downs, in improvement may be achieved for buildings by the self-centering response of post-tensioned walls.

This high-rise CLT building is assumed to be constructed in a metropolis where has a large demand for housing but

shortage of land resource, for example, Shanghai in China. Therefore, a normal residential building in Shanghai with three apartments per story of around 100 m² each [3] is regarded as the reference in this paper. The layout of the designed high-rise CLT building, shown in Figure 3, is simplified from the building in Shanghai. It neglects some interior details but modified two half cores [3] into a full core for more stiffness. Height of the timber building is estimated at 132 m, with an identical story height of 3.3 m

(including floor). The floor plan dimensions are 33.7 m in X-axis by 15.7 m in Y-axis (Figure 3). The thicknesses of core walls are also divided into four groups like the PT bars, respectively 350 mm, 300 mm, 250 mm and 200 mm for 0-10, 11-20, 21-30 and 31-40 stories. The thickness of CLT sidewalls of 300 mm is consistent throughout the whole building, and so is the thickness of floors of 250 mm.

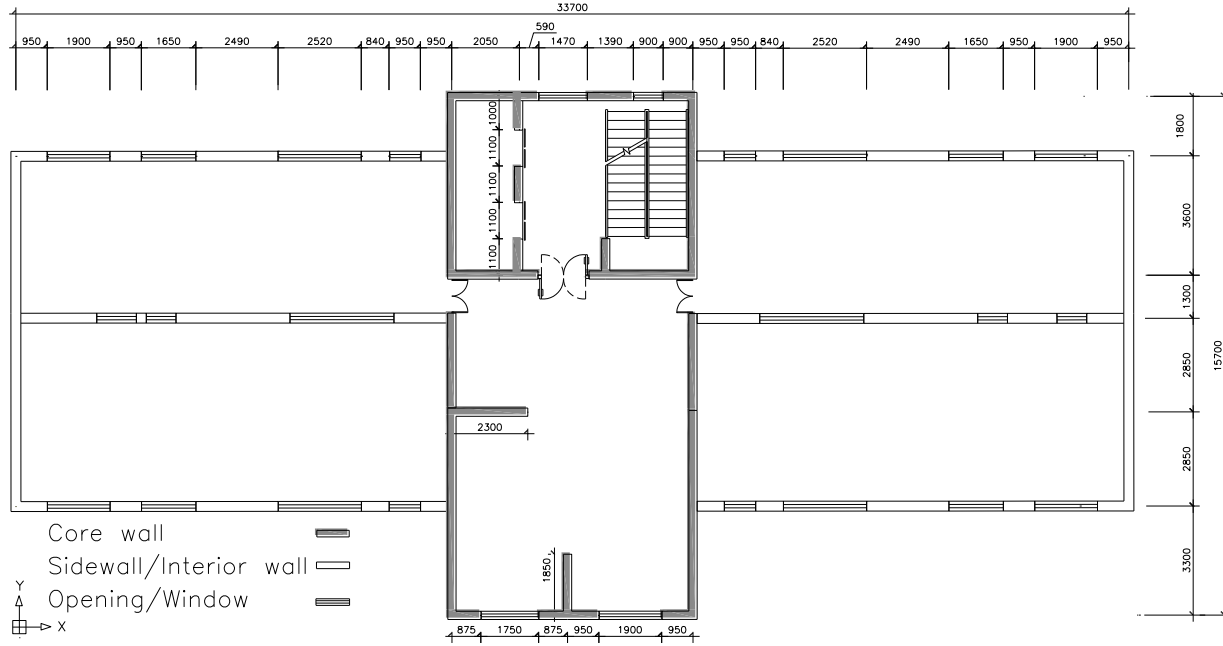


Figure 3: Preliminary floor layout of the CLT tall building

2.2 STRUCTURAL MATERIALS

By counteracting the tensile stresses induced by horizontal loads with the stresses induced by prestressing, the building stiffness is increased, decreasing horizontal deflection. The employed high strength steel material conforms to the requirement of ASTM Designations A722 [14]. Its minimum ultimate strength is 1035 MPa, and the minimum yield stress is accordingly 80% of the minimum ultimate tensile strength of the bars (i.e. 828 MPa).

The major strength and stiffness direction of CLT generally corresponds to the grain orientation of the outer layers. While Blass and Fellmoser [15] recommend also considering cross layers loaded perpendicular to the grain to avoid large discrepancies between calculation and test results. They proposed an approach by using composition factors to take rolling shear into account, so that homogenized solid wood panels with cross layers into a one-layer homogeneous orthotropic material. Mechanical properties of CLT panels were estimated in accordance

with DIN 1052: 2008 [16] and DIN EN 1194 [17] as well as CLT manufacturers. On the basis of the characteristic values of strength class GL28 for Glulam, effective moduli for CLT panels are accordingly figured out (Table 1). The values of $E_{0,ef}$ and $E_{90,ef}$ are respectively defined for walls in two plane directions and, for floors in two directions out of the plane. The characteristic values of tensile and compressive strength of wall panels are 16.5 N/mm² and 24 N/mm².

Table 1: Modulus of elasticity (MoE) of homogenized CLT panels [N/mm²]

CLT panel (loading type)	$E_{0,ef}$	$E_{90,ef}$
Wall (in-plane)	10200	2900
Floor (out of the plane)	11700	1300

2.3 DESIGN LOADS

Horizontal forces result from wind load is generally the governing factor in the design of tall and slender buildings, as they are strongly sensitive to wind-excited oscillation. Although wind load is a kind of dynamic load, it is treated as static here by multiplying the gust effect factor at the primary stage, and also in consideration of simplification and feasibility. Based on Chinese standard GB50009-2001 [18], a 50-year return-period wind pressure of Shanghai is used here. The calculated effective wind pressures increase along the increment of the building's height, from the ground level of 0.49 kN/m^2 to the top of the building of 1.87 kN/m^2 . No safety factor has been applied on these values.

When dead load and live load are combined with the wind load, the maximum compression stress can be determined using the appropriate load combination factors. The design of post-tensioned CLT wall (to ultimate limit state and serviceability limit states) could be in accordance with Eurocode 5 [19]. In order to fully understand the behaviour of post-tensioned structures, a transient analysis should be made, taking into account creep and relaxation effects. In this paper only short term analyses are made to verify the feasibility.

3 FINITE ELEMENT MODEL

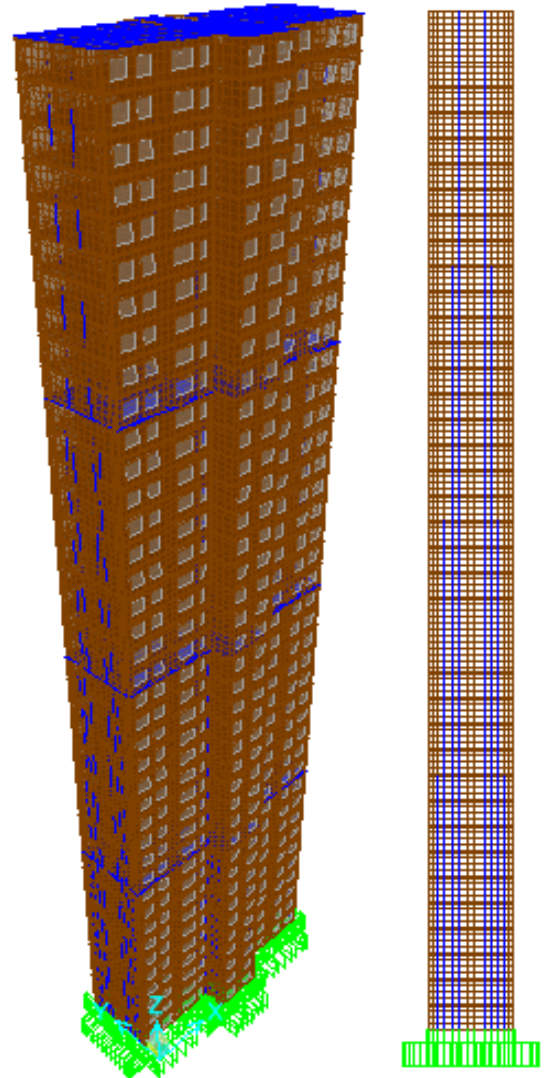
3.1 FE MODEL OF STRUCTURAL MATERIALS

Nonlinear finite element analyses have been executed to investigate the behavior of CLT buildings with prestressing. The SAP2000[®] program is utilized for analysing the behavior of structural components and whole constructions throughout the current study.

CLT panels are modelled as orthotropic shell elements for the finite element analysis. The E-moduli values presented in Table 1 are defined for the shell elements in the SAP2000. Concrete outriggers are modelled with homogeneous shell element with the E-modulus of 30000 MPa .

As the steel bars are not bonded with CLT panels, cable element is used to model PT bars under tension in the finite element model. The cable is non compressive or bending element, and therefore can only carry tension forces. At the base of the wall, the cable element nodes are assumed to be fixed to the foundation. The top nodes of cable elements are constrained to the concrete outrigger element nodes, to model the anchorages at outrigger levels. Therefore, the movement of the top nodes of cable elements would keep identical with the displacement of the shell elements nodes at concrete outriggers. Figure 4 displays a 3D view of the finite element model of the designed full CLT building and in Y-axis located CLT wall with cable elements. The cable elements are concentrated in one location in the model for ease of programming and calculation, but in reality will be

placed around the circumference. The forces and stresses are assumed to be evenly distributed over the CLT walls.



(a) 3D view of the FE model of CLT building

(b) CLT wall with unbonded PT bars in Y-axis in right side

Figure 4: FE model of CLT building with unbonded PT bars, which are modelled by cable element (gap links are not in the view)

The post-tensioning of the CLT wall should be equilibrated by compressive forces in wall members, which is produced by tensile forces in the unbonded PT bars. The tensile forces are simulated in the FE model by applying a certain temperature decrease that produces a corresponding thermal strain by steel contraction. A temperature change of ΔT produces axial thermal strain in the cable element, which can be computed as equation (1):

$$\Delta L = \alpha L_0 \Delta T \quad (1)$$

where α is the coefficient of thermal expansion which is $1.2 \times 10^{-5} \text{K}^{-1}$ for steel, and L_0 is initial length of steel bar.

According to the Hooke's law, the extensional strain of steel bars can be calculated by dividing the tensile stress by the Young's modulus in the elastic portion as expressed in equation (2):

$$\varepsilon = \frac{\sigma}{E} = \frac{F/A_0}{E} \quad (2)$$

where $\varepsilon = \Delta L/L_0$, F is the force exerted on an steel tendon under tension, and A_0 is the original cross-sectional area of steel bar.

Since the end nodes of cable elements are rigidly connected with nodes of shell element of concrete outriggers, there is no relative movement between these nodes. The changed temperature of equation (3) can therefore be derived directly from equations of (1) and (2) as:

$$\Delta T = \frac{F}{\alpha E A_0} \quad (3)$$

3.2 FE MODEL OF GAP LINKS

Besides post-tensioning bars in the vertical direction, all other joints are included in the model. The next important simulation aspect deals with the connections in the horizontal planes. They are modelled as gap-links. A nonlinear gap property is specified for the local 1 axis of gap links, which is in the global Z direction of the model. The opening displacement for the gap is set to zero, so that the gap link is in compression only in its local 1 axis. No tension load can be taken up. Furthermore, linear elastic properties, i.e., linear shear stiffnesses are specified for the local axes 2 and 3.

For the purpose of avoiding the excessive number of links, a reduced number of equivalent connections is introduced in the model.

As a simplification, the number of links in each story is reduced as follows:

- 10 gap links to connect one core wall in X-axis with the floor – S_{cx} ;
- 10 gap links to connect one core wall in Y-axis with the floor – S_{cy} ;
- 10 gap links to connect one sidewall in X-axis with the floor – S_x ;
- 10 gap links to connect one sidewall in Y-axis with the floor – S_y ;
- 5 linear spring links to connect two orthogonal walls in the corner – CO;
- 5 linear spring links to connect sidewall in X-axis with core wall – SC.

Secondly, as presented earlier, the building is divided into four sections: story 1–10, 11–20, 21–30 and 31–40. The stiffness of each link type in one section is defined with the maximum stiffness value of these ten stories.

Lastly, the floor slabs, which deflect negligibly under in-plane loading while comparing to wall deformations, are assumed as rigid diaphragms without any spring links between each other.

3.3 PRE-ANALYSIS

A first numerical analysis of the building was performed with rigid connections, i.e. without considering the effect of reduced stiffness of the mechanical fasteners, and no prestressing applied. This allows a direct comparison to a full concrete model. In addition, it allows a first estimate of the tensile forces under extreme wind loads.

First of all, the maximum bending and axial compression have been checked by the analysis results. The axial compressive stress produced by dead and live load in this model without prestressing forces is computed for about 2 MPa both of core wall and sidewall located on the ground floor. Meanwhile, additional flexural compressive stresses resulting from bending moments are 4.1 MPa and 3.5 MPa respectively for core wall and sidewall at the foundation. The axial compressive stresses combined with the flexural compressive stresses result in maximum stresses. The resulting stress of 6.1 MPa for core wall is at such a level the prestressing could be applied. Here a sensitivity analysis can be performed.

Secondly, the tensile forces (F_t) caused by wind load were derived from the analysis results. The values (Table 2) are also used as effective prestressing forces (F_p) that are exerted to unbonded PT bars. The required minimum diameters (\varnothing_{\min}) of the unbonded PT bars that used in every ten stories are also determined referring to ASTM standard [12]. Furthermore, the forces, i.e. equivalent lowering temperatures, that will be assigned to the cable elements in the advanced simulation model are determined in accordance with equation (3) and are also reported in Table 2.

Table 2: Applied design values in every ten stories and the equivalent prestressing forces

Story	1-10	11-20	21-30	31-40
Core wall				
F_t (F_p) [kN]	3250	1980	918	232
\varnothing_{\min} [mm]	65 × 2	65	46	26
ΔT [°C]	-204	-250	-230	-182
Sidewall				
F_t (F_p) [kN]	1860	982	379	--
\varnothing_{\min} [mm]	65	46	32	--
ΔT [°C]	-234	-246	-197	--

The distributed wind loads obtained from the pre-analysis of this basic model have been used to determine the required fasteners (Table 3) and their stiffness. The required numbers of fasteners (per meter), is indicatively given in Table 3 assuming 4 mm screws are applied.

Table 3: Distributed lateral load and linear shear stiffness.

Story	1-10	11-20	21-30	31-40
Core wall				
V_y [kN]	1182	986	733	393
S_{cy} [kN/mm]	157	142	104	53
Screw Nr. [/m]	36	33	24	13
Sidewall				
V_y [kN]	608	567	449	257
S_y [kN/mm]	81	75	60	34
Screw Nr. [/m]	29	27	21	12

The abovementioned assumptions and basic values from the rigid model are applied in the further analysis.

4 ANALYTICAL RESULTS OF THE ADVANCED MODEL

4.1 COMPARISON OF VIBRATION FREQUENCIES

Here are three models that have been analysed: an advanced CLT model considering gap links, a rigid CLT model and a rigid concrete model. They share the exact same lay-out and are all applied with same prestressing. The latter two models don't take the influence from mechanical fasteners into account and therefore have been analysed here as reference and comparison systems.

It is known that the natural frequency of a structure is dependent on two system properties: mass and stiffness. Generally, buildings with higher natural frequencies have larger stiffness and tend to smaller lateral displacements. The first three mode shapes are usually the most important for high-rise buildings, so that their eigenfrequencies are summarized in Table 4. The first and second vibration modes of these three models listed in Table 4 are translation modes, respectively along the Y-axis (short side of the building) and the X-axis (long side). The third vibration shape rotates about the Z-axis.

Table 4: Frequencies for the first three modes of vibration, in Hz

	1 st Mode	2 nd Mode	3 rd Mode
Direction	Bending Y-axis	Bending X-axis	Torsional
Concrete model	0.37	0.71	1.4
Rigid CLT model	0.33	0.43	0.5
Advanced CLT model	0.26	0.32	0.38

The eigenperiod of a building can be estimated with a commonly used formula [11]: $T = H / 46$ with H the height of the building. For this building an eigenfrequency of 0.35 Hz is consequently found, overestimating the value of the advanced CLT model but in good agreement with the others. This reflects smaller stiffness of the advanced CLT model than the rigid CLT model, while these two models have almost the same mass.

4.2 VERIFICATION OF THE COMBINED STRESSES

In order to compensate the tensile stress on CLT walls caused by wind load in the weak direction, unbonded PT bars are implemented individually along the long edges of the building. When the tensile forces have been counteracted by the prestressing forces in the windward, the compressive stress of the UPT CLT wall will be considerably increased in the leeward side. Therefore, the combined stresses of the advanced model are verified at this side of the building.

According to the values of prestressing forces illustrated in the Table 2 the compression stress on the leeward side of the wall are calculated at 3.3 MPa of the core wall and 3.1 MPa of the sidewall. To these, the bending stresses caused by the wind load are added. The compression stresses are calculated in section 3.3 as 4.1 MPa for core wall and 3.5 MPa for side wall respectively. Consequently, combined maximum compression stress at the foundation is 7.4 MPa for the core wall, which is an acceptable value, considering the fact that no safety factor has been applied on the 1.87 kN/m^2 as given in paragraph 2.3.

4.3 HORIZONTAL DISPLACEMENTS

Because the planar structure of the building is not strictly symmetrical, The CLT wall at the right side (Figure 4) takes up slightly higher forces, and thus deflects slightly larger than the wall at the left side. The maximum displacement is therefore read from the top node of the right side wall.

The top displacement of the rigid CLT model with prestressing under the load combination (WLD) consisting of wind (W), live (L) and dead (D) load is calculated at about 335 mm (Table 5). As presented in the preceding section, the rigid CLT model overestimates the stiffness of the structure, resulting in smaller displacements. When considering the influence of mechanical connections, i.e. using nonlinear gap links to simulate the connections in the advanced model, the top displacement increases to approximately 760 mm in the nonlinear analysis of the load combination of WLD. It can therefore be concluded that utilizing appropriate spring elements in the FE model to simulate mechanical connections is necessary for a better understanding of the lateral behavior of tall CLT buildings.

It needs to be emphasized that load combination factors have not been taken into account in load combinations applied here. In that case the expected geometrical nonlinear effects will diminish.

Table 5: Displacements of the rigid and advanced CLT models under different load cases, in mm

Load case	Rigid CLT model	Advanced CLT model
WLD	335	762
WLD (P-Δ)	346	--
WPLD	318	525
WPLD (P-Δ)	332	--

Further adding the prestressing (P) load to the load combination of WLD forms a new one as WPLD. The top displacements under WPLD now reduce to 318 mm and 525 mm respectively of the rigid CLT model and the gap linked advanced CLT model (Figure 5).

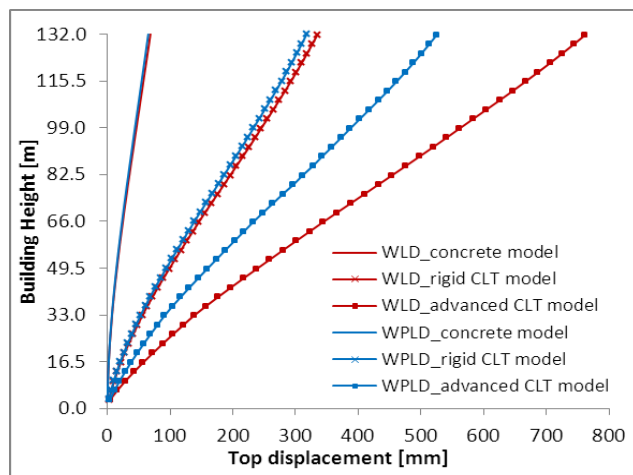


Figure 5: Displacements of the rigid CLT model under wind load and the advanced model under different load cases

When geometrical nonlinearity is taken into account in the calculation, the top deflection of the structure increases by about 3-4% for the rigid model, implying such an effect is small for a full CLT building. However, for the advanced model the analysis is still in progress. The result also reveals that the prestressing effect is more clearly and realistically expressed in the advanced model. It can also be concluded that additional prestressing has positive effect on reducing the horizontal sway. The lateral behavior of the advanced model is closer to the expected scenario. Further research by performing a sensitivity analysis of the model for different horizontal – vertical load combinations and different levels of prestress will allow for a better understanding of the lateral behavior of the high-rise CLT buildings.

Although the present result of top displacement still exceeds the limit value of several existing regulations, the

positive influence and effect from unbonded PT bars is quite encouraging and has potential for further improving the whole lateral resisting performance of CLT high-rise buildings and save in the vertical connections.

The fact that the CLT building would exceed sway requirements is not relevant at this stage. The model is developed in order to make a sensitivity analyses for different options and to be able to compare the results with an existing building. The model can be used to analyse the effect of measures such as increasing building width, increased amount of shear walls, or increasing the stiffness of existing shear walls. It depends on the strategy of the designer what he can and would apply in realistic application.

5 SUMMARY AND OUTLOOK

This paper introduced a design-based numerical model that uses finite element method to estimate the lateral load behavior of high-rise CLT buildings with unbonded bars in the facade. Results from the advanced model and a fully rigid model are compared.

It is concluded that, the advanced model with nonlinear gap links is able to rationally simulate the CLT structure. The number and strength of horizontal mechanical joints are mainly decided by the lateral load, especially the wind load in this research case. The utilization of unbonded PT bars has been proved to effectively decrease the lateral displacement of the high-rise CLT building, by about 30%. This reduction clearly relates to the building lay-out and cannot be assumed as a general value. However, compared to a concrete and/or rigid model, the horizontal deflections are much larger, indicating that a complex model is indeed needed, when predicting deflections.

Further research will focus on developing and modifying the current model in order to be able to perform parameter studies with regard to the joints, the materials used and their cross section. In addition, time dependent properties will be implemented to see how stresses develop over time and what the consequences for the building stiffness will be. In addition, the location and the efficiency of outriggers will be subject of further analysis.

REFERENCES

- [1] Harris M.: Wood goes high-rise. *Engineering & Technology*, 7:43-45, 2012.
- [2] Smith I. and Frangi A.: Overview of design issues for tall timber buildings. *Structural Engineering International*, 18:141-147, 2008.
- [3] Van De Kuilen J.W., Ceccotti A., Xia Z., and He M.: Very Tall Wooden Buildings with Cross Laminated Timber. *Procedia Engineering*, 14:1621-1628, 2011.
- [4] Ceccotti A., Follesa M., Kawai N., Lauriola M., Minowa C., Sandhaas C.: Which seismic behaviour factor for multi-storey buildings made of cross-

- laminated wooden panels. In: *39th CIB W18 Meeting*, No. 39-15. Firenze, Italy, 2006.
- [5] Ceccotti A.: New technologies for construction of medium-rise buildings in seismic regions: the XLAM case. *Structural Engineering International*, 18:156-165, 2008.
- [6] Ceccotti A., Sandhaas C., and Yasumura M.: Seismic Behaviour of Multistory Cross-laminated Timber Buildings. In: *the International convention of Society of Wood Science and Technology*. Geneva, Switzerland, 2010.
- [7] Kurama Y., Pessiki S., Sause R., and Lu L.-W.: Seismic behavior and design of unbonded post-tensioned precast concrete walls. *PCI journal*, 44(3):72-89, 1999.
- [8] Kurama Y., Sause R., Pessiki S., and Lu L.-W.: Lateral load behavior and seismic design of unbonded post-tensioned precast concrete walls. *ACI Structural Journal*, 96(4), 1999.
- [9] Serrano E.: Documentation of the Limnologen project: overview and summaries of sub projects results. 2009.
- [10] Serrano E.: Limnologen—Experiences from an 8-storey timber building. In: *15th International wood construction conference*. Garmisch, Germany, 2010.
- [11] Smith B. S. and Coull A.: Tall building structures: analysis and design. John Willey & Sons, Inc., New York, USA, 1991.
- [12] Nigel Priestley M. J., Sritharan S., Conley J. R., and Pampanin S.: Preliminary results and conclusions from the PRESSS five-story precast concrete test building. *PCI journal*, 44(6):42-67, 1999.
- [13] Laursen P. T. and Ingham J. M.: Structural testing of single-storey post-tensioned concrete masonry walls. *The Masonry Society Journal*, 19(1):69-82, 2001.
- [14] ASTM Designation: A 722/A 722M-98: Standard Specification for uncoated high-strength steel bars for prestressing concrete. 2003.
- [15] Blass H. J. and Fellmoser P.: Design of solid wood panels with cross layers. In: *8th World Conference on Timber Engineering*, 14(17.6). Lahti, Finland, 2004.
- [16] DIN 1052: Entwurf, Berechnung und Bemessung von Holzbauwerken - Allgemeine Bemessungsregeln und Bemessungsregeln für den Holzbau, in German, 2008.
- [17] DIN EN 1194: Brettschichtholz - Festigkeitsklassen und Bestimmung charakteristischer Werte, in German, CEN, 1999.
- [18] GB 50009-2001 (2006): Load code for the design of building structures, in Chinese, 2006.
- [19] EN 1995-1-1:2004 (E), Eurocode 5: Design of timber structures – Part 1-1: General rules and rules for buildings. CEN, 2004.